

H14-196

SO₂ EFFECT ON SECONDARY ORGANIC AEROSOL FORMATION: EXPERIMENTAL AND MODELLED RESULTS

Manuel Santiago¹, Marta G. Vivanco¹ and Ariel F. Stein²

¹Unidad de Modelización y Ecotoxicidad de la Contaminación Atmosférica. Departamento de Medio Ambiente. CIEMAT. Av. Complutense, 22. 28040, Madrid. Spain

²Earth Resources & Technology on assignment to NOAA's Air Resources Laboratory, Silver Spring, MD. EEUU

Abstract: The effect of SO₂ in the photooxidation of a mixture of anthropogenic precursors is studied. For that purpose, five experiments with a mixture of 1,3,5-trimethylbenzene, o-xylene, toluene and octane in the presence of HONO were carried out in the EUPHORE outdoor chamber by adding different initial SO₂ concentrations in each experiment. The experimental secondary organic aerosol obtained in the experiments was compared with the aerosol simulated by two air quality models (CMAQ and CHIMERE) under the same initial conditions. A simplified version of the models was designed in order to consider the closed system of the chamber, where only gas phase chemistry and aerosol formation take place.

While the experimental results show a clear increase of the aerosol formed in the presence of increasing SO₂ concentrations, the models do not consider this enhancement in the simulations. The behaviour of the models points out the need of a way to implement this SO₂ effect on anthropogenic secondary organic aerosol.

Key words: *air quality modelling, SOA formation, acidic effect, CMAQ, CHIMERE*

INTRODUCTION

Secondary organic aerosols (SOA) are considered to account for a major fraction of the total atmospheric aerosol. These secondary organic particles are formed through the degradation of certain volatile organic compounds (VOCs), which undergo several oxidative processes to generate a set of products with a volatility that can be low enough to partition to the particle phase and therefore produce SOA. Although considerable advances have been achieved in the understanding of the chemistry behind SOA formation and its implementation in air quality models, there are still gaps to cover in order to provide consistent SOA formation simulations in these models.

One of the key aspects to take into account is the particle phase chemistry. Although the reactions that take place in the particle phase are not as well known as the gas phase oxidation reactions, there is evidence of their effect on the SOA formation. Among these reactions, there is an important group of heterogeneous acid-catalyzed reactions, in which oxygenated compounds formed through gas phase oxidation react in the presence of sulfuric acid particles to form low volatility products that increase the total SOA mass of the system [Jang et al., 2002; Jang and Kamens, 2001].

In order to study the effect of these acid-catalyzed reactions in a mixture of anthropogenic VOCs, five photooxidation experiments were carried out in the EUPHORE outdoor chamber, adding different initial SO₂ concentrations in each experiment. Special versions of the CMAQ and CHIMERE air quality models were applied, in order to evaluate model SOA formation in the presence of SO₂.

EXPERIMENTAL PROCEDURE

Five experiments were carried out in the EUPHORE smog chamber (Valencia, Spain) in order to analyze the effect of an increase of initial SO₂ concentration on the SOA formed from the oxidation of certain anthropogenic precursors. A mixture of 1,3,5-trimethylbenzene (TMB), o-xylene (OXYL), toluene (TOL) and octane (OCT) was introduced into the chamber, and nitrous acid (HONO) was used as the oxidant agent. Further description of the experiments can be seen in [Vivanco et al., 2011a; Vivanco et al., 2011b]

The EUPHORE facility consists in a half-spherical teflon chamber with a volume of approximately 200 m³, and it has been previously described by other authors [Volkamer et al., 2001]. Once the reactants have been introduced, the chamber is opened to sunlight so that the photochemical processes take place and SOA starts to be formed. Initial experimental conditions are summarized in Table 1.

Table 1. Initial conditions of the photooxidation experiments in the EUPHORE chamber.

| | TMB (ppb) | TOL (ppb) | OXYL (ppb) | OCT (ppb) | HONO (ppb) | NO (ppb) | NO ₂ (ppb) | SO ₂ (ppb) | RH (%) | T (K) |
|------|--------------|--------------|---------------|--------------|---------------|-------------|--------------------------|--------------------------|-----------|----------|
| (A1) | 171 | 101 | 25 | 88 | 99 | 19 | | | 19-10 | 296-305 |
| (A2) | 160 | 107 | 26 | 89 | 89 | | | 17 | 18-9 | 298-307 |
| (A3) | 116 | 84 | 18 | 72 | 57 | 182 | 128 | 514 | 47-62 | 299-297 |
| (A4) | 204 | 106 | 23 | 87 | 89 | 126 | 36 | 582 | 16-25 | 302-307 |
| (A5) | 155 | 100 | 24 | 85 | 94 | 15 | | 790 | 9-4 | 299-307 |

Although initial conditions for the five experiments were planned to be similar (with the exception of SO₂ concentration), unfortunately some NO and NO₂ were also introduced into the chamber in some experiments (A4 and A5), due to the chemical synthesis of HONO.

Aerosol concentration was monitored using a Scanning Mobility Particle Sizer (SMPS) with a 5 min scan rate. The SMPS includes a particle counter (TSI 3022A CPC) and a differential mobility analyzer (TSI 3081 DMA). The SMPS measures number and volume concentrations as well as particle size distributions.

Over the course of the experiments two fans located on the floor of the chamber help to homogenize the mixture. Aerosol concentrations were corrected for particle losses by measuring the concentration decay after the closure of the chamber. Once the chamber is closed, it can be assumed that no more aerosol is formed and, therefore, the decay observed on the mass and volumetric concentrations can be attributed to the particle losses, mainly because of wall deposition.

The inorganic content of the aerosol was determined by analytical methods described in a previous paper [Vivanco et al., 2011b]. Table 2 summarizes the nitrate and sulfate content in the experiments.

Table 2. Inorganic characterization (expressed as %) of the filtered aerosol mass collected in the experiments.

| | (A1) | (A2) | (A3) | (A4) | (A5) |
|----------------------|-------|--------|----------|---------|-------|
| Nitrates (%) | 4-8.5 | 2.5-5 | 1.7-2.1* | 1.7-2.1 | 1-2.5 |
| Sulphates (%) | 1-2.0 | 4-10.5 | 28-31* | 28-31 | 33-44 |

* As no filter was available, values for A4 were used.

The nitrates and sulfates detected in the filters may be originated from the aqueous equilibrium of HNO₃ and H₂SO₄ formed in the gas phase. Nitric acid is formed through several gas phase reactions involving NO_x, while sulfuric acid is formed from SO₂ in the presence of OH radicals.

SMPS temporal profiles

Temporal profiles of the total secondary aerosol collected and the SOA (obtained by discounting the sulfate and nitrate content to the total aerosol) for the five experiments are presented in Figure 1. The temporal profiles are obtained from the SMPS volumetric data considering an aerosol density of 1.3 g·cm⁻³.

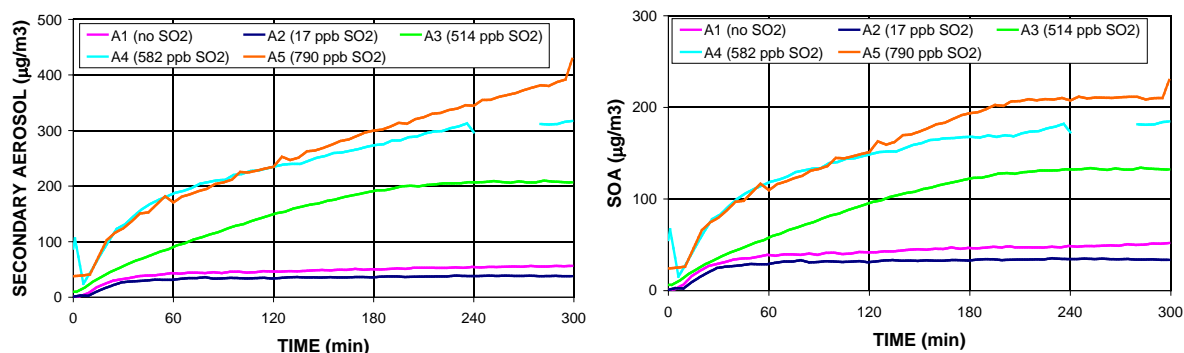


Figure 9. Total secondary aerosol (left) and SOA (right) for the whole set of experiments. SOA is obtained by discounting the sulfate and nitrate content to the total aerosol

There is no substantial difference between total aerosol and SOA for the experiments A1 and A2, due to the inexistence or very low initial SO₂ concentration. However, for the rest of the experiments a high increase of both total and organic secondary aerosol is observed, due to the noticeable presence of H₂SO₄ in the particle phase, enhancing organic particle production. When looking at the right side of Figure 1, it can be seen that no SOA increase is obtained when less than 20 ppb SO₂ are introduced (the aerosol produced in A2 is similar to that in A1). However, at higher SO₂ concentrations, SOA increases as the initial SO₂ does. Nevertheless, the difference on SOA formation between experiments A3 and A4 may be attributed not only to the different SO₂ introduced, but also to differences in initial reactant concentrations, with higher initial NO_x in A3. In this sense, some authors [Ng et al., 2007] have reported higher SOA concentrations at low NO_x conditions from aromatic compounds. In any case, both, A3 and A4 experiments present higher SOA concentration than those with no or low SO₂.

The results presented in Figure 1 can be explained by an enhancement of the SOA produced by the aromatic VOCs and octane oxidation in acidic conditions, provided by the presence of H₂SO₄. This SOA enhancement may be explained by acid-catalyzed particle phase reactions of small carbonyls such as glyoxal or methylglyoxal (formed during the photooxidation of aromatic compounds) which form oligomers in the particle phase and therefore increase the SOA mass [Jang et al., 2002].

MODEL PERFORMANCE

Specific versions of CHIMERE (2008c) and CMAQ (v4.7) were prepared in order to emulate the closed system represented by the EUPHORE chamber, where transport, dispersion and deposition processes are not present. Because of this, the models

were simplified to consider only gas phase chemical processes and aerosol formation, disabling all the other processes that have relevance in a real atmosphere. SOA formation reactions in the models are coupled with gas-phase chemical mechanisms so that the chemistry of the two phases is related. The gas-phase chemical mechanisms used are MELCHIOR2 (in CHIMERE) and SAPRC-99 (in CMAQ).

In order to consider the effect of the temperature and the relative humidity over the course of the simulations, hourly values measured in the chamber during the experiment were used. Both models were run for the five experiments, using the initial conditions given in Table 1.

The inorganic sulphates and nitrates as well as the SOA simulated by the models were compared with the experimental data.

Inorganic aerosol simulation results

For experiments A2, A3, A4 and A5 an estimation of the inorganic sulfates and nitrates in the aerosol phase was done by taking into account the characterization presented in Table 2. The experimental temporal profiles of this inorganic mass (obtained as the sum of sulfates or nitrates) were compared with the inorganic aerosol species simulated by CMAQ and CHIMERE. Both models consider the uptake to the particle phase of the gaseous HNO_3 and H_2SO_4 to form nitrate aerosol (ANO3 in CMAQ and pHNO3 in CHIMERE) and sulfate aerosol (ASO4 in CMAQ and pH2SO4 in CHIMERE).

Therefore, the inorganic mass simulated by CMAQ (ANO3 + ASO4) and CHIMERE (pHNO3 + pH2SO4) are compared with the experimentally estimated sulfate and nitrate aerosol. Results are shown in Figure 2.

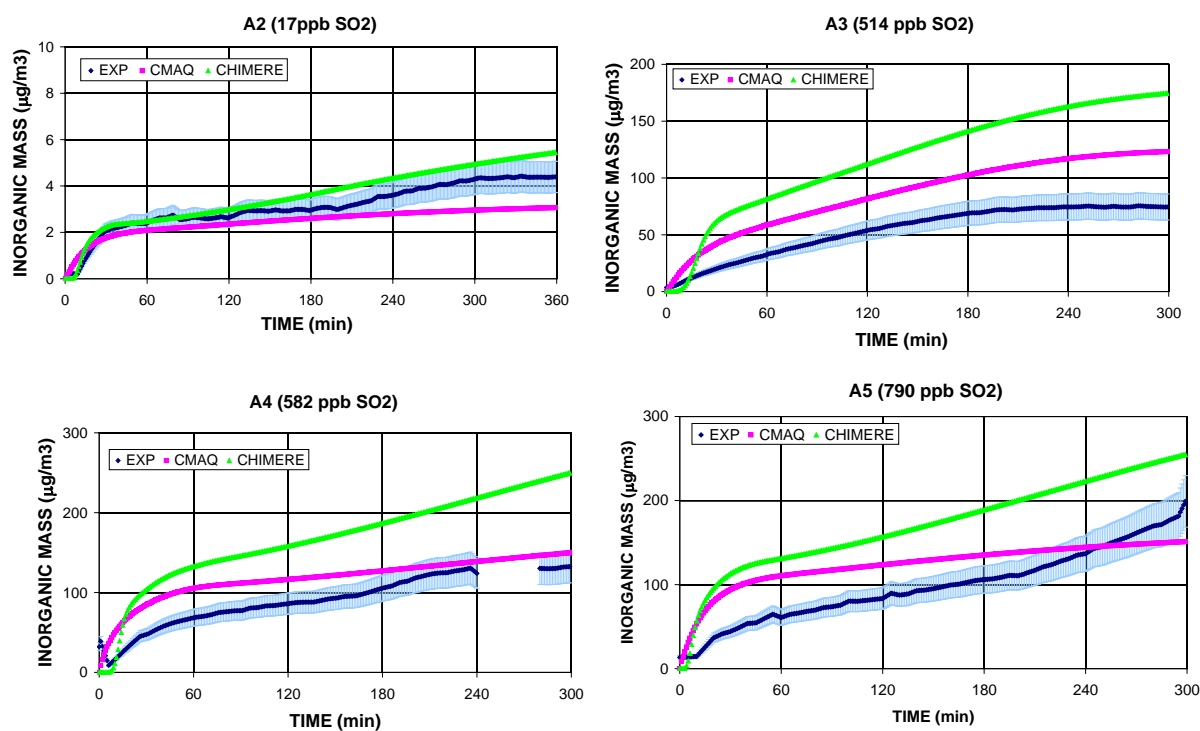


Figure 2. CMAQ (pink squares), CHIMERE (green triangles) and measured with SMPS (assuming an aerosol density of $1.3 \text{ g}\cdot\text{cm}^{-3}$) inorganic mass concentration. Vertical light blue lines in SMPS concentration illustrate the concentration mass range of the aerosol for a particle density range of $1.1 - 1.5 \text{ g}\cdot\text{cm}^{-3}$.

The largest fraction of the inorganic aerosols according to both models is formed by sulphates. In the experiment with low initial SO_2 both models perform quite well, by reproducing observed data. When initial SO_2 is introduced, some overprediction is observed, especially for the CHIMERE model, showing a significant deviation in some experiments. Regarding experiment A3, it must be taken into account that sulphate and nitrate content was taken from experiment A4, with similar initial SO_2 concentration, as no filter was available. This assumption adds more uncertainty to the inorganic estimation, and therefore the overall results presented in Figure 2 should be taken as approximated.

SOA simulation results

In CMAQ, SOA parameterization is based on the differentiation between semivolatile and nonvolatile SOA [Carlton et al., 2010]. SOA species formed from the VOCs employed in this study are the semivolatile AALK (long alkanes SOA), ATOL1 and ATOL2 (SOA from high yield aromatics such as toluene), AXYL1 and AXYL2 (SOA from low yield aromatics such as

xylenes and trimethylbenzenes). Nonvolatile species ATOL3, AXYL3 (SOA from aromatic photooxidation in a low-NO_x environment) and AOLGA (SOA formed through oligomerization processes) are also considered.

In CHIMERE model, SOA is formed through the partition of semivolatile species into two different particle phases, an organic phase and an aqueous phase, depending on their hydrophobic or hydrophilic nature [Pun et al., 2002]. In this case, SOA is formed by three hydrophilic species: AnA0D (nondissociative compounds), AnA1D (single dissociative compounds) and AnA2D (double dissociative compounds), and two the hydrophobic SOA species: AnBIP low VP_{sat} compounds (low vapor pressure compounds) and AnBmP (medium vapor pressure compounds).

A comparison between the SOA simulated with CMAQ and CHIMERE models and measured with SMPS (discounting the inorganic fraction) is presented in Figure 3.

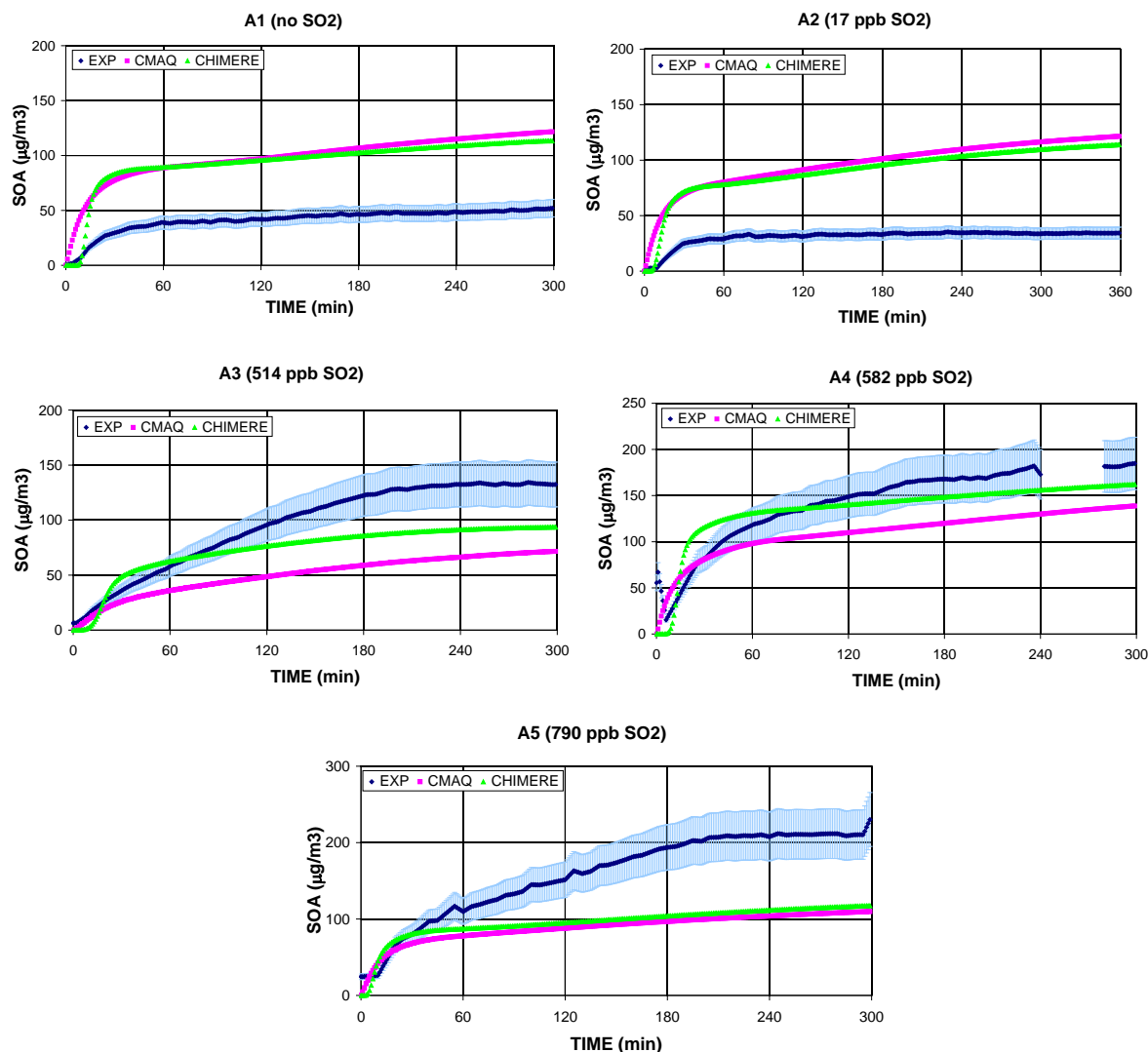


Figure 3. CMAQ (pink squares), CHIMERE (green triangles) and SMPS (blue, assuming an aerosol density fo $1.3 \text{ g}\cdot\text{cm}^{-3}$)SOA. Vertical light blue lines illustrate the concentration mass range of the aerosol for a density range of $1.1 - 1.5 \text{ g}\cdot\text{cm}^{-3}$.

Two different responses of the models can be distinguished in Figure 3. First, for the experiments A1 and A2 both CHIMERE and CMAQ overpredict the SOA produced in the chamber. The overprediction in these experiments is a factor of 2 and even higher, and seems to be related with the empirical nature of the parameters that govern SOA formation in the models, which do not represent accurately the conditions of these experiments. Some research is currently being done to investigate the reasons of this overestimation.

The second behaviour is observed in experiments A3, A4 and A5, where the high initial SO₂ leads to an increase of the SOA formed in the chamber. In this experiments the response of the models is the opposite, underpredicting the aerosol formed, although CHIMERE provides a reasonable agreement in A3 and A4.

Figure 4 shows the SOA concentration modelled in the five experiments for the CMAQ (left side of the figure) and CHIMERE (right side) models. It can be seen that CMAQ presents a range of variation wider than CHIMERE. For SOA, and

in these experiments, CHIMERE results are in a better agreement with observations. Nevertheless, both models seem to better perform in the experiments A3 and A4 (initial SO₂ values around 500 ppb), while overestimate observations at low initial SO₂ values (A1, A2) and underestimate observations at the highest SO₂ values (790 ppb, A5).

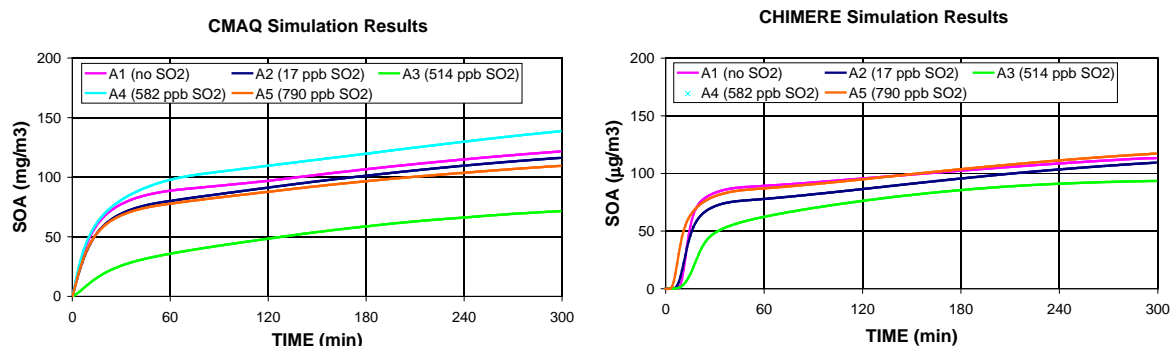


Figure 4. CMAQ (left) and CHIMERE (right) SOA simulation results for the five experiments.

With the exception of the CMAQ simulation for A3, it can be seen how for the two models the SOA predicted in the five experiments is very similar. These results support the idea that the models are not considering the influence of SO₂ in the SOA formed from anthropogenic precursors.

CMAQ predicts a lower SOA in A3 due to the implementation in its code of the results presented by Ng et al. (2007) and discussed in the SMPS temporal profiles presented above.

CONCLUSIONS

SOA formation from the anthropogenic precursors presented in this study is enhanced by the presence of SO₂ in the system. This enhancement has been previously attributed to acid-catalyzed particle phase reactions that lead to the formation of polymers and produce an increase of the total organic aerosol mass. While the uptake of gaseous H₂SO₄ to the particle phase is a well known process already implemented in air quality models, CMAQ and CHIMERE are not considering the influence of the SO₂ effect on SOA formation, at least for the aromatic compounds presented here and for the octane. The implementation of this effect is a crucial issue in order to improve SOA representation in the models, as SO₂ is an important pollutant in most urban areas.

ACKNOWLEDGEMENTS

This study has been financed by the Spanish Science and Innovation Ministry (CGL2008 02260/CLI) and the Spanish Ministry of Environment. We gratefully acknowledge all the EUPHORE team members.

REFERENCES

- Carlton, A., Bhawe, P., Napelenok, S., Edney, E., Sarwar, G., Pinder, R., Pouliot, G. and Houyoux, M., 2010. Model Representation of Secondary Organic Aerosol in CMAQv4.7, *Environmental Science and Technology*, 44, 8553–8560
- Jang, M., Czoschke, N.M., Lee, S. and Kamens, R.M., 2002. Heterogeneous Atmospheric Aerosol Production by Acid-Catalyzed Particle-Phase Reactions, *Science*, 298, 814-817
- Jang, M. and Kamens, R.M., 2001. Atmospheric Secondary Aerosol Formation by Heterogeneous Reactions of Aldehydes in the Presence of a Sulfuric Acid Aerosol Catalyst, *Environmental Science and Technology*, 35, 4758-4766
- Ng, N.L., Kroll, J.H., Chan, A.W.H., Chhabra, P.S., Flagan, R.C. and Seinfeld, J.H., 2007. Secondary organic aerosol formation from m-xylene, toluene, and benzene, *Atmospheric Chemistry and Physics*, 7, 3909-3922
- Pun, B.K., Griffin, R.J., Seigneur, C. and Seinfeld, J.H., 2002. Secondary organic aerosol 2. Thermodynamic model for gas/particle partitioning of molecular constituents, *Journal of Geophysical Research*, 107,
- Vivanco, M.G., Santiago, M., Borrás, E., Sánchez, M., Clavero, M.Á., Ródenas, M., Alacreu, F. and Stein, A.F., 2011a. Experimental data on SOA formation for anthropogenic and biogenic mixtures of organic gases, Short communication submitted to *Atmospheric Environment* on July 20th 2011,
- Vivanco, M.G., Santiago, M., Martínez-Tarifa, A., Borrás, E., Ródenas, M., García-Diego, C. and Sánchez, M., 2011b. SOA formation in a photoreactor from a mixture of organic gases and HONO for different experimental conditions, *Atmospheric Environment*, 45, 708-715
- Volkamer, R., Platt, U. and Wirtz, K., 2001. Primary and Secondary Glyoxal Formation from Aromatics: Experimental Evidence for the Bicycloalkyl-Radical Pathway from Benzene, Toluene, and p-Xylene, *Journal of Physical Chemistry A*, 105, 7865-7874